Underground Wireless Communications for Monitoring of Drag Anchor Embedment Parameters: A Feasibility Study

Alvin Valera Hwee-Pink Tan
Institute for Infocomm Research (I2R)
1 Fusionopolis Way, #21-01 Connexis, Singapore 138632
Email:{acvalera, hptan}@i2r.a-star.edu.sg

Ma Xiaoping
National University of Singapore
21 Lower Kent Ridge Rd, Singapore 119077
Email: u0607129@nus.edu.sg

***Abstract*—In the offshore engineering community, reliable deep-water anchor performance is critical for mooring floating platforms such as Mobile Offshore Drilling Units. In a typical installation, an anchor is fully embedded into the seabed (up to 100 m). This has to be done with high fidelity as anchor failure can cause floating units to go adrift, damaging oil and gas pipelines. The likelihood of this happening may be reduced with a data acquisition system comprising various sensors/measurement instruments housed in the anchor, where their data is then transmitted in some ways towards the seabed, and then onwards to the installation vessel. In this paper, we explore the feasibility of electromagnetic wave underground wireless communications as a low cost means to transmit key anchor parameters from the anchor to the seabed. We employ two semi-empirical models to obtain the path loss characteristics at different operating frequencies and volumetric water contents.**

***Keywords*-Underground through-soil wireless communications; drag anchor embedment monitoring; empirical modeling.**

I. Introduction

In the offshore engineering community, reliable deep-water anchor performance is critical for mooring floating Mobile Offshore Drilling Units (MODUs). Drag embedment anchors (DEAs) are the most utilized anchor for mooring floating MODUs in the Gulf of Mexico. DEA installation typically consists of applying a pre-determined load to the mooring line to fully embed the anchor into the seabed (up to 100 m penetration depth). This installation process has to be done with high fidelity as anchor failure can result in MODUs going adrift and colliding with production structures and/or dragging anchors and damaging oil and gas pipelines or sub-sea production systems.

For example, during hurricanes Ivan, Katrina, and Rita, 24 MODUs experienced mooring system failures due to anchor failures [1]. Anchors were dragged during some of these MODU mooring failures and are suspected to have caused several instances of pipeline damage that in turn led to delays in restoring oil and gas production after the hurricanes. There were at least four instances of failures during hurricane Ike that resulted in MODUS leaving stations.

Recently, R. Ruinen [2] proposed a newly developed DEA data acquisition system that allows key anchor parameters to be viewed real time on the installation vessel, resulting in a higher confidence level with regards to anchor installation. The system comprises a load measuring anchor shackle connecting the mooring line to the anchor, inclinometers to measure anchor orientation and pressure sensors to measure anchor depth. The off-the-shelf sensors are housed in a watertight canister in the anchor, where their data is combined with a processor, and transmitted by means of an umbilical cable to a sub-sea modem located above the seabed, which in turn transmits the data to the vessel. This will enable the installation contractor to determine, at an early stage, if changes to the installation are required. This process is illustrated in Fig. 1.

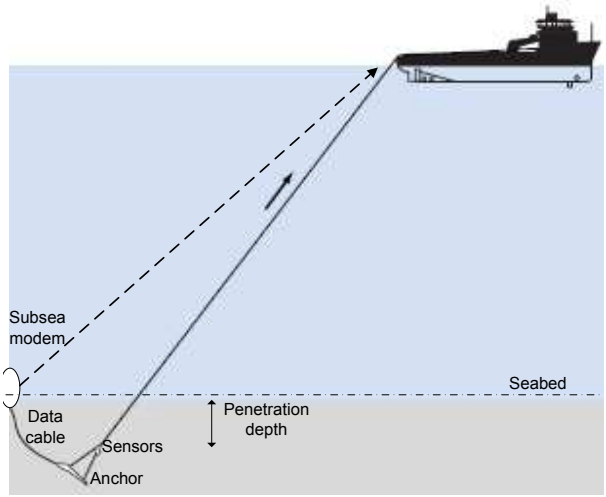

Figure 1. Illustration of installation of Drag Embedment Anchors [3].

However, the cable is prone to damage during the installation process, and may be costly due to the penetration depth. Hence, in this paper, we explore the feasibility of *electromagnetic wave* underground wireless communications as a *low cost* means to transmit key anchor parameters from the anchor to the seabed. This paper is organized as follows: Section II describes related work and in Section III, the characteristics of the underground channel are analyzed. In

Section IV, we present some numerical results to quantify the feasibility of underground wireless communications for the dissemination of DEA parameters. Finally, we conclude and outline items for future work in Section V.

II. Related Work

Unlike terrestrial and underwater wireless sensor networks, wireless underground sensor networks is a relatively new field and can rely on (i) *through-air*, (ii) *through-soil* wireless communications or (iii) a combination of both. In [4], the authors introduced the concept of wireless underground sensor networks, provided an extensive overview of applications and challenges, and suggested various physical layer techniques, including electromagnetic wave propagation, for through-soil communications.

In [5], the authors performed a detailed characterization of electromagnetic wave communications through soil, focusing on the significant attenuation caused by soil. Numerical analysis suggests that communications is feasible (up to a few meters) using electromagnetic waves in the 300–900 MHz range, and communication success increases with decreasing operating frequency and decreasing water content in soil. In addition, a *single* (two-path) model is suitable to characterize communications for *low-depth* ($>$2 meters depth) deployments. The authors followed on with experimental measurements using Mica2 sensor motes [6] that operate at 433 MHz in [7]. The observations agree with the channel model presented in [5]. Specifically, it was shown that (i) the orientation of the underground nodes plays an important role in wireless connectivity, (ii) the burial depth is important, and (iii) the wireless underground channel exhibits temporal stability.

The above works suggest that commodity sensor motes that operate in the 300–900 MHz range are not suited for our applications, where a communication range of the order of 100 m is required. Moreover, while underground through-soil electromagnetic wave communications with a ground/air interface is considered previously, we investigate the feasibility of through-soil electromagnetic wave communications with a *ground/water* interface for our application. Although commercial radio frequency-based products, e.g., Seatext modem [8], that can achieve through-soil communications of up to 100 m are available, we restrict our investigations to low cost, low frequency radio modems, e.g., Radiometrix modems [9].

III. Through-Soil Communications Using EM Waves

In this section, we modify the underground channel model proposed by Li *et al.* [5] for our application scenario, where through-soil wireless communications is required from the embedded anchor and a receiver at the seabed/water interface, as depicted in Fig. 2.

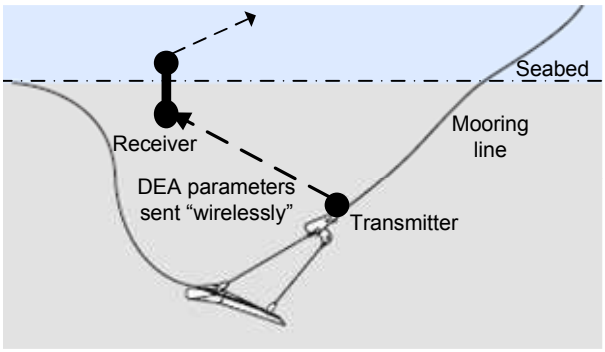

Figure 2. Through-soil wireless communication system for monitoring of DEA. A sensor node is attached to the DEA which periodically transmits DEA parameters to a receiver at the seabed/water interface.

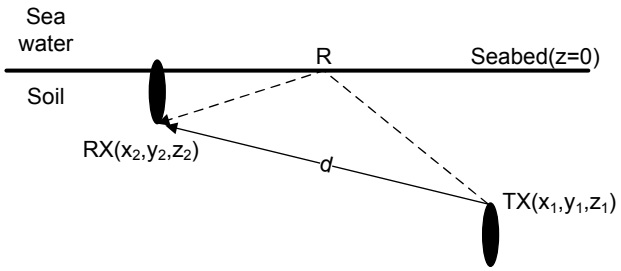

Figure 3. Electromagnetic wave propagation for underground through-soil communications.

According to [5], electromagnetic wave propagation through-soil comprises of signal contributions from the (i) *direct path*, (ii) *indirect path* due to reflection from seabed, and (iii) *multipath fading* as a result of impurities in the soil, as illustrated in Fig. 3. In the following discussions, we describe the details of each of these components.

A. Direct Path

In the direct path, the signal propagation between the sender and receiver suffers from path loss, L_p (in dB), given as follows [5]:

$$L_p = 6.4 + 20log(d) + 20log(\beta) + 8.69\alpha d \qquad (1)$$

where d refers to the distance between the sender and the receiver in meters. This formulation essentially combines the free-space and dielectric losses. The quantities α and β are components of the electromagnetic wave propagation constant $\gamma = \alpha + j\beta$ where α is known as the *attenuation constant* (in Nepers/meter) while β is the *phase constant* (in radians/meter) [10]. These quantities are dependent on the relative complex dielectric permittivity of the medium, ϵ_r, which is defined as

$$\epsilon_r = \epsilon' - j\epsilon'' \qquad (2)$$

The quantity ϵ' is the *real dielectric permittivity* while ϵ'' is the *imaginary dielectric permittivity*. If μ_0 is the magnetic permeability of free space, ϵ_0 is the permittivity of free space, then the attenuation constant and phase constant can be obtained as

$$\alpha = \omega \sqrt{\frac{\mu_0 \epsilon_0 \epsilon'}{2} \left[\sqrt{1 + \left(\frac{\epsilon''}{\epsilon'} \right)^2} - 1 \right]} \quad (3)$$

$$\beta = \omega \sqrt{\frac{\mu_0 \epsilon_0 \epsilon'}{2} \left[\sqrt{1 + \left(\frac{\epsilon''}{\epsilon'} \right)^2} + 1 \right]} \quad (4)$$

In this paper, we will employ two *semi-empirical models*, namely the Peplinski Model [11] and Topp Model [12], to predict the path loss in soil at various frequencies and volumetric water contents. The paper by Li *et al.* [5] used the Peplinski Model to determine the path loss and bit error rate as a function of frequency, volumetric water content, and soil composition. The disadvantage of the model is that it is only applicable for the frequency range from 300 MHz to 1.3 GHz. As this range of frequencies is not suitable for long range transmission [5], we investigate the path loss and bit error rate performance at lower frequencies. To accomplish this, we employ the Topp Model which can be used from 1 to 1000 MHz.

1) Peplinski Model: The Peplinski Model [11] belongs to a class of models that use the relative amounts of soil constituents and their individual dielectric characteristics to obtain the dielectric properties of a soil mixture. In particular, this model considers the soil composition (fraction of sand, clay or silt) and volumetric water content. The expressions for the real and imaginary parts of the relative permittivity are given as follows:

$$\epsilon' = 1.15[1 + \frac{\rho_b}{\rho_s}(\epsilon_s)^{\alpha'} + \theta^{\beta'}(\epsilon_{f_w})^{\alpha'} - \theta]^{1/\alpha'} - 0.68 \quad (5)$$

$$\epsilon'' = \left[\theta^{\beta''} (\epsilon''_{f_{ws}})^{\alpha'} \right]^{1/\alpha'} \quad (6)$$

As mentioned, the model can only be used for the frequency range from 300 MHz to 1.3 GHz. In the above equations, the quantity ρ_b is the bulk density in grams/cm^3, $\rho_s = 2.66$ g/cm^3 is the specific density of the solid soil particles, $\alpha' = 0.65$ (empirically determined), θ is the volumetric water content of the soil, and ϵ_s is the relative permittivity of the host (soil solids) [13] which can be obtained as follows:

$$\epsilon_s = (1.01 + 0.44\rho_s)^2 - 0.062 \quad (7)$$

The quantities β' and β'' are empirically determined constants which depend on the mass fraction of sand, S, and the mass fraction of clay C:

$$\beta' = 1.2748 - 0.519S - 0.152C \quad (8)$$

$$\beta'' = 1.33797 - 0.603S - 0.166C \quad (9)$$

The real and imaginary parts, ϵ'_{f_w} and ϵ''_{f_w}, of the relative dielectric constant of water are given by Eqs. (10) and (11), respectively [13]:

$$\epsilon'_{f_w} = \epsilon_{w\infty} + \frac{\epsilon_{w0} - \epsilon_{w\infty}}{1 + (2\pi f \tau_w)^2} \quad (10)$$

$$\epsilon''_{f_w} = \frac{2\pi f \tau_w (\epsilon_{w0} - \epsilon_{w\infty})}{1 + (2\pi f \tau_w)^2} + \frac{\sigma_{m_v}}{2\pi \epsilon_0 f} \quad (11)$$

where ϵ_{w0} is the static dielectric constant for water, $\epsilon_{w\infty} = 4.9$ is the high-frequency limit of ϵ'_{f_w}, τ_w is the relaxation time for water, f is the frequency, and σ_{m_v} is the effective conductivity of water in Sm^{-1}. However, to account for the effective conductivity of the soil mixture in water, Eq. (11) is modified and the resulting quantity, which we denote by $\epsilon''_{f_{ws}}$, is given by the following equation [11]:

$$\epsilon''_{f_{ws}} = \frac{2\pi f \tau_w (\epsilon_{w0} - \epsilon_{w\infty})}{1 + (2\pi f \tau_w)^2} + \frac{\sigma_{eff}}{2\pi \epsilon_0 f} \frac{(\rho_s - \rho_b)}{\rho_s m_v} \quad (12)$$

The quantity σ_{eff} is the effective conductivity of soil in Sm^{-1} which also depends on the mass fraction of clay and sand and is given by the following equation:

$$\sigma_{eff} = 0.0467 + 0.2204\rho_b - 0.4111S + 0.6614C$$

2) Topp Model: The Topp Model [12] is a widely used model in soil science for determining the volumetric water content, θ, of a given soil sample [14]. Normally, the apparent relative permittivity, K_a, of the soil is measured using a measurement technique known as time domain reflectometry (TDR). K_a is then used to obtain θ using the following third order polynomial:

$$K_a = 3.03 + 9.3\theta + 146\theta^2 - 76.7\theta^3 \quad (13)$$

This relation has been obtained by Topp, *et al.* [12] from extensive TDR measurements carried over a wide variety of soil mixtures. The model has a wider frequency range compared to the Peplinski Model, from 1 to 1000 MHz and volumetric water content range from 0 to 55% [14]. To obtain α and β, we use the relation

$$K_a = \frac{\epsilon'}{2} \sqrt{1 + \sqrt{1 + \left(\frac{\epsilon''}{\epsilon'} \right)^2}} \quad (14)$$

For this model, ϵ'' is defined as $\sigma/\omega\epsilon_0$ where σ is the ionic conductivity of soil. In the literature, the ratio between the imaginary and real components of the relative permittivity, $\epsilon''/\epsilon' = \tan\delta$, is known as the loss tangent. Note that K_a

is a factor of Eq. (4). Hence, it is obvious that β can be expressed in terms of K_a as follows:

$$\beta = \omega\sqrt{\mu_0\epsilon_0 K_a} \tag{15}$$

After β is obtained, α can then be easily derived using the relation in [10]:

$$\alpha = \frac{\omega^2\mu_0\epsilon_0\epsilon''}{2\beta} \tag{16}$$

For convenience and easy reference, we provide a summary of all the quantities that have been used in the preceding discussion. To eliminate confusion on the various permittivity variables, we denote the relative permittivity of soil as $\epsilon_{soil} = \epsilon'_{soil} + j\epsilon''_{soil}$ and the relative permittivity of water as $\epsilon_{fw} = \epsilon'_{fw} + j\epsilon''_{fw}$. Table I summarizes the list of notations, their descriptions, units as well as default values (whenever applicable).

B. Reflected Path from Seabed

Assume sender TX is located at (x_1, y_1, z_1), and receiver RX at (x_2, y_2, z_2) (see Fig. 3). The coordinates of the reflection point, R, $(x_r, y_r, 0)$[1] can be evaluated using Eqs. (17) and (18)[2].

$$x_r = \frac{-n_2 \pm \sqrt{n_2^2 - 4n_1n_3}}{2n_1} \tag{17}$$

$$y_r = m_1x_r + m_2 \tag{18}$$

where

$$\begin{aligned}
m_1 &= \frac{y_2 - y_1}{x_2 - x_1} \\
m_2 &= y_1 - m_1x_1 \\
n_1 &= (z_1^2 - z_2^2)(1 + m_1^2) \\
n_2 &= n'_2 - n''_2 \\
n_3 &= n'_3 - n''_3 \\
n'_2 &= z_1^2(-2x_2 + 2m_1m_2 - 2y_2m_1) \\
n''_2 &= z_2^2(-2x_1 + 2m_1m_2 - 2y_1m_1) \\
n'_3 &= z_1^2(x_2^2 + m_2^2 - 2y_2m_2 + y_2^2) \\
n''_3 &= z_2^2(x_1^2 + m_2^2 - 2y_1m_2 + y_1^2)
\end{aligned}$$

Since $x_1 < x_r < x_2$, a unique solution for x_r always exists from solving Eq. (17), which leads to a unique solution for y_r as well. According to [5], the reflected path from the seabed introduces a path loss component (in dB) given by $V_{dB} = 10\ \log(V)$, where V can be obtained from the following equation:

$$\begin{aligned}
V^2 &= 1 + (\Gamma e^{-\alpha\Delta r})^2 - 2\Gamma e^{-\alpha\Delta r} \\
&\times \cos\left[\pi - \left(\phi - \frac{2\pi}{\lambda}\Delta r\right)\right],
\end{aligned} \tag{19}$$

where Δr is the path length difference between the direct and reflect paths, and Γ and ϕ refer to the magnitude and the phase angle of the complex reflection coefficient at the reflection point R, respectively. The quantity $\Gamma e^{j\phi}$ is given by

$$\Gamma e^{j\phi} = \frac{\eta_{water} - \eta_{soil}}{\eta_{water} + \eta_{soil}} \tag{20}$$

Here, η is the complex intrinsic impedance of the medium, which is given by

$$\eta = \sqrt{\frac{\mu}{\epsilon' - j\epsilon''}}$$

C. Rayleigh Fading Model

While time-varying multipath fading occurs due to random air refraction with time in terrestrial wireless communications, this does not occur in underground through-soil communications since the medium (composition of soil) is relatively stable with time [5]. In fact, this temporal stability has been verified by Silva and Vuran [7].

In the context of the application which is the seabed, the presence of rocks, clay particles, and other objects can incur reflection and refraction for electromagnetic waves, giving rise to multi-path characteristics in *location* instead of time. In other words, for a fixed inter-node distance, the received signals are *different* at different locations, and obey the Rayleigh probability distribution.

D. Bit Error Rate

We quantify the fidelity of through-soil wireless communications in terms of the Signal-to-Noise Ratio (SNR) and Bit Error Rate (BER). If P_t is the transmit power (in dBm), and P_n is the ambient noise power (in dBm), then the SNR (in dB) can be evaluated as

$$SNR = P_t - L_f - P_n$$

where L_f (in dB) is the total path loss, taking into account the effects of the direct and reflected paths, and is given as follows:

$$L_f = L_p - V_{dB} \tag{21}$$

The BER depends on the modulation scheme that is employed by the radio modem. In this paper, we calculate the BER using 2-PSK as it is the simplest and most error-robust phase-shift keying modulation. The BER of 2-PSK is given by

$$BER = \frac{1}{2}\text{erfc}(\sqrt{SNR}) \tag{22}$$

[1]The plane $z = 0$ is assumed to be the seabed.

[2]These equations are not applicable when $z_1 = z_2$ or $x_1 = x_2$. However, it is easy to obtain the corresponding solutions for these two particular cases.

Table I
SOIL AND SEAWATER PARAMETERS.

Notation	Description (units)	Default Value
μ	Magnetic permeability (Hm^{-1})	$4\pi \times 10^{-7}$
ρ_b	Bulk density ($\mathrm{g}cm^{-3}$)	1.5
ρ_s	Specific density of solid soil particles ($\mathrm{g}cm^{-3}$)	2.66
τ_w	Relaxation time of water (sec)	9.231×10^{-12}
σ_{mv}	Effective conductivity of water ($\mathrm{S}m^{-1}$)	0
σ_{eff}	Effective conductivity of soil ($\mathrm{S}m^{-1}$)	
ϵ_0	Permittivity of free space	8.854×10^{-12}
$\epsilon'_{soil} + j\epsilon''_{soil}$	Complex relative dielectric constant of soil	
ϵ_s	Relative permittivity of host	
$\epsilon'_{fw} + j\epsilon''_{fw}$	Complex relative dielectric constant of water	
ϵ_{w0}	Static dielectric constant of water	80.1
$\epsilon_{w\infty}$	High frequency limit of ϵ'_{fw}	4.9
θ	Volumetric water content	
S	Mass fraction of sand	
C	Mass fraction of clay	

IV. NUMERICAL RESULTS

In this section, we evaluate the relationship between path loss and bit error rate with various parameters for the (i) single (direct) path model, and (ii) two-path (direct+reflected) model using the Qualnet [15] network simulator for our DEA monitoring application. We specifically investigate the impact of operating frequency and volumetric water content.

In the simulations using the Peplinski Model, it has been assumed that $S = 50\%$, $C = 15\%$, $\rho_b = 1.5$ g/cm^3, $\theta = 25\%$, $2\pi\tau_w = 0.58 \times 10^{-10}$ s, $\sigma_{m_v} = 0$ Sm^{-1}, and $\epsilon_{w0} = 80.1$ unless otherwise noted.

A. Impact of Frequency on Path Loss

Figure 4 shows the single (direct) path loss characteristics as the distance is varied from 1 to 30 m and the frequency of operation is varied from 300 to 700 MHz for the Peplinski model (Fig. 4(a)) and 1 to 700 MHz for the Topp model (4(b)). These results are obtained using $\theta = 25\%$.

A quick comparison of the results show that the two models provide relatively close path loss predictions at short distances and at frequencies around 700 MHz. However, as the frequency decreases to 300 MHz, the difference increases especially at higher distances. This difference can be attributed to the different formulations of the two models.

In general, the results indicate that path loss increases as the frequency of operation increases. At a distance of 30 m, a signal at 700 MHz suffers more than 700 dB of attenuation. In contrast, a signal at 1 MHz is only reduced by 54 dB. Other frequencies close to 1 MHz likewise suffer lower attenuation. At 5 and 10 MHz, signal attenuation is at 120 and 140 dB, respectively. It is therefore clear that to achieve long-range signal propagation, low frequencies close to 1 MHz must be used, as high frequencies can experience extreme path loss.

B. Impact of Volumetric Water Content

Figure 5 shows the single (direct) path loss per meter as the volumetric water content θ is varied from 5 to 50% and the frequency of operation is varied from 300 to 700 MHz for the Peplinski model (Fig. 5(a)) and 1 to 700 MHz for the Topp model (Fig. 5(b)). We anticipate that for the DEA monitoring application, the water content will be higher as seabed soil has higher water content compared to terrestrial soil. Thus, our simulations show θ up to 50%, higher than the 25% used in previous studies [5], [4].

Comparing the results for the frequency range from 300 to 700 MHz from the two models, we can see that the path loss values are relatively close especially at lower θ values. At 5% water content, both models predict a loss of around 10 dB/m. At 50% water content, the Topp Model has slightly lower path loss at lower frequencies (*i.e.*, at 300 MHz.) compared to the Peplinksi Model. Note that at 300 MHz, Topp predicts a loss of around 28 dB/m while Peplinski predicts 30 dB/m.

The results clearly indicate the severe impact of water content on the signal attenuation. All frequencies are affected, with the higher frequencies exhibiting higher increase in signal attenuation. At 700 MHz, path loss dramatically increases from 12 dB/m to around 40 dB/m as the water content increases from 5% to 50%. Meanwhile at 1 MHz, path loss shows a slight increase from 1 dB/m to 3 dB/m as the water content increases from 5% to 50%. Frequencies close to 1 MHz also exhibit lower increase in signal attenuation. At 5 and 10 MHz, path loss increases from 2 and 3 dB/m to 6 and 8 dB/m, respectively, as the water content increases from 5% to 50%. Once again, these results suggest that the use of low frequencies close to 1 MHz can help achieve low path loss even at high soil water content.

C. Impact of Signal Reflection

From the preceding results, it is clear that for long-range transmission, operating frequencies above 100 MHz

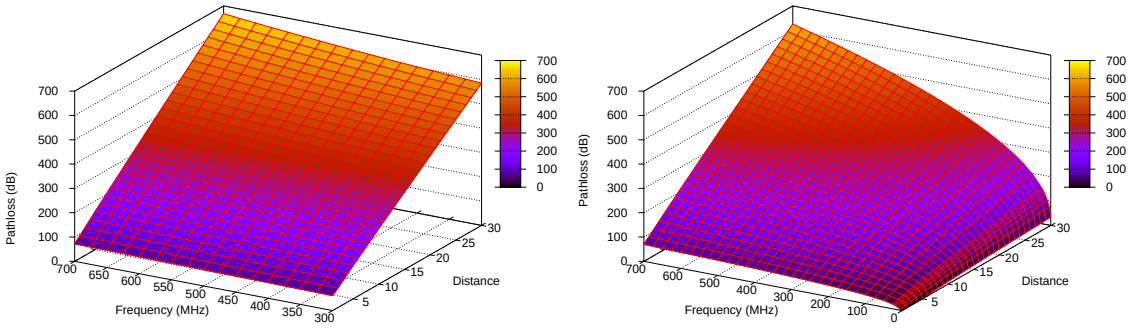

(a) Peplinski Model (b) Topp Model

Figure 4. Numerical simulation results showing the effect of frequency on single (direct) path loss as distance is varied from 1 to 30 m.

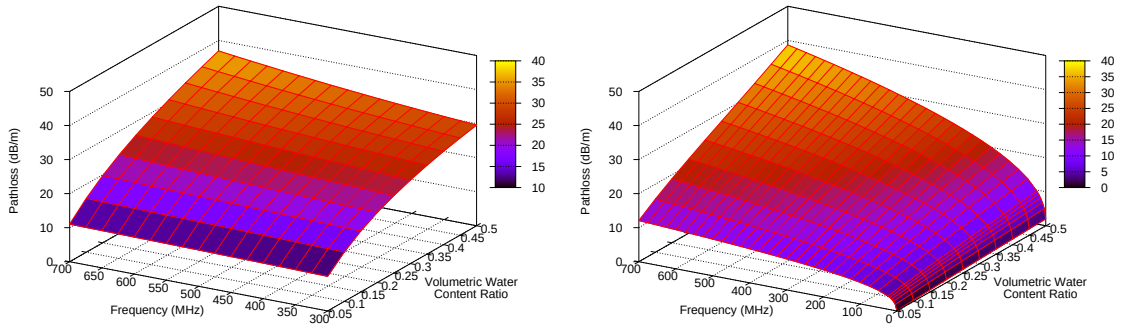

(a) Peplinski Model (b) Topp Model

Figure 5. Numerical simulation results showing the effect of volumetric water content on single (direct) path loss as operating frequency is varied from 1 to 700 MHz.

are not suitable as they can be subjected to extreme signal attenuation. We therefore focus our analysis on the frequency range from 1 to 100 MHz (obtained using the Topp Model) as it exhibits low path loss even when the water content is at 50%. We now consider the effect of signal reflection on the path loss characteristics using two deployment scenarios.

Fig. 6(a) shows the path loss when the sender and receiver are buried at the same depth which is varied from 0.2 to 10 m. Fig. 6(b) shows the path loss when the receiver is buried at 0.2 m and the sender's burial depth is varied from 0.2 to 10 m. Note that in both scenarios, the horizontal distance between the sender and receiver is fixed at 10 m. Note that the first scenario is not really practical for DEA monitoring as the sender and receiver are both deeply buried. The second scenario is more useful as the sender is buried deeper than the receiver. The results show that the signal reflection affects only the first scenario (Fig. 6(a)). Even so, the effect is not significant and is only noticeable on the higher frequencies. We can therefore safely disregard the impact of signal reflection in further analysis.

D. Bit Error Rate

Fig. 7 shows the 2-PSK bit error rates as the sender to receiver distance is varied from 1 to 100 m and computed using Eq. (22). Fig. 7(a) shows the BER for the frequencies 1, 10, 20, 50, and 100 MHz at volumetric water content $\theta = 25\%$ and transmit power $P_t = 0$ dBm. The plot clearly shows that at frequencies above 10 MHz, the BER approaches 50% (*i.e.*, $\log 0.5 = -0.3$) *even* at very short distances. At 100 MHz for instance, the BER is already 50% at just around 6 m. At 50 and 20 MHz, the BER is 50% at around 8 and 14 m, respectively. At 10 MHz, a distance of 20 m is reached before the BER reaches 50%. These results suggest that to achieve low BER at higher distances (and therefore achieve long-range transmission), we have to transmit at 1 MHz. Note that at this frequency, the BER reaches 50% only at around 90 m.

We now take a closer look at the effect of volumetric water content on the BER when the operating frequency

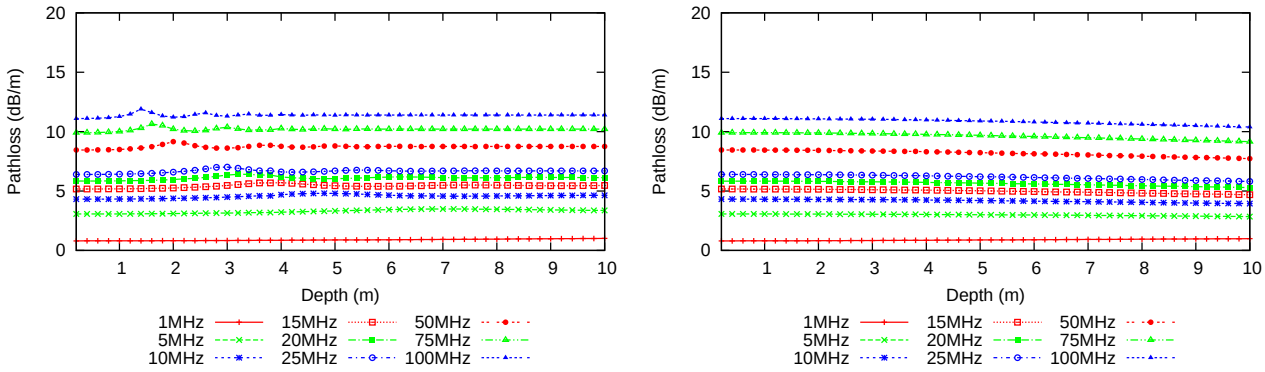

(a) Sender and receiver at same burial depth

(b) Sender and receiver at different burial depths

Figure 6. Numerical simulation results showing the effect of signal reflection at various operating frequencies (Horizontal distance between sender and receiver is 10 m.

is fixed at 1 MHz. Fig. 7(b) shows the BER for $\theta = \{10, 20, 30, 40, 50\}\%$ and $P_t = 0$ dBm. We can observe the severe impact of water content on the BER. At 10%, the BER is extremely low (not shown in the Figure.) However, as the water content increases, the BER performance degrades substantially. At 20%, the BER reaches close to 50% at around 100 m. At 50%, the BER reaches 50% at around 50 m. These results highlight an uncertainty on the real-world performance of the DEA monitoring system especially since the seabed soil is anticipated to be water-saturated.

The previous BER results are obtained when the transmit power P_t is fixed at 0 dBm. To know the improvement in BER that can be achieved when P_t is varied, we present a plot showing the BER for $P_t = \{0, 5, 10, 15, 20, 25\}$ dBm in Figs. 7(c) and 7(d) where θ is 0.25 and 0.5, respectively. As expected, an increase in transmit power results in a decrease in BER. To achieve a relatively low BER of 10^{-5} at 100 m and $\theta = 25\%$, the transmit power must be set to at least 25 dBm (or 100 mW). However, at $\theta = 50\%$, note that even at 40 dBm (10 W), the achievable distance where BER is still acceptable (i.e., $\leq 10^{-5}$) is at most 70 m.

V. Conclusions and Future Work

In the offshore engineering community, reliable deep-water anchor performance is critical for mooring floating platforms such as Mobile Offshore Drilling Units. In a typical installation, an anchor is fully embedded into the seabed which can penetrate up to a depth of 100 m. To reduce anchor failures which can cause substantial damage to floating units as well as gas and oil pipelines, a real-time DEA monitoring system has been proposed. In such a system, data acquisition instruments comprising various sensors/measurement instruments are housed in the anchor and sensor readings are transmitted in some ways towards the seabed, and then onwards to the installation vessel.

In this paper, we explored the feasibility of employing electromagnetic wave underground wireless communications as a low cost means to transmit key anchor parameters from the anchor to the seabed. We employed two semi-empirical models to determine the path loss characteristics of electromagnetic waves as they propagate in an underground setting. Our numerical simulation results show that electromagnetic waves can experience severe attenuation at higher frequencies and higher volumetric water content. A signal transmitted at a frequency of 1 MHz and power of 40 dBm can only be received (and decoded with high probability) at a distance of 70 m when the soil water content is at 50%.

Achieving 100 m range is difficult even at 1 MHz when the soil water content is extremely high. In our future work, we will investigate the use of a multi-hop topology wherein additional nodes are deployed (e.g., by attaching them along the mooring lines) to act as relays or intermediaries. In such a system, the sender node will send sensor readings to the nearest relay node instead of sending directly to the receiver at the seabed.

References

[1] A. Cruz and E. Krausmann, "Damage to offshore oil and gas facilities following hurricanes katrina and rita: An overview," *Journal of Loss Prevention in the Process Industries*, vol. 21, no. 6, pp. 620–626, 2008.

[2] R. Ruinen, "Monitoring of drag anchor embedment parameters," in *Proceedings of Deep Offshore Technology Asia Pacific Conference*, Dec. 2008.

[3] Vryhof Anchors, "Anchor manual," [Online]. Available: http://www.vryhof.com [Accessed: January 20, 2010].

[4] I. F. Akyildiz and E. P. Stuntebeck, "Wireless underground sensor networks: Research challenges," *Ad Hoc Networks*, vol. 4, no. 6, pp. 669–686, Jul. 2006.

[5] L. Li, M. C. Vuran, and I. F. Akyildiz, "Characteristics of underground channel for wireless underground sensor networks," in *Proceedings of the Sixth IFIP Annual Mediterranean Ad Hoc Networking WorkShop*, Jun. 2007, pp. 92–99.

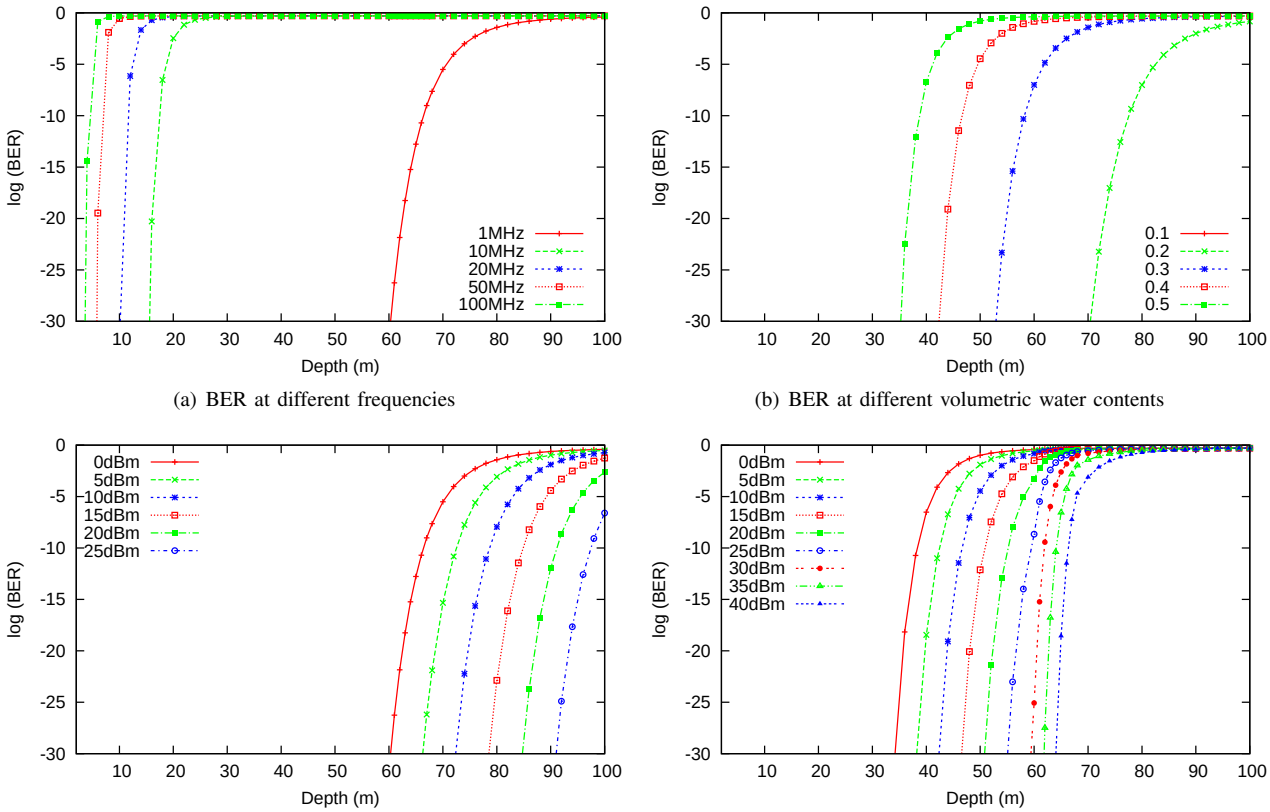

(a) BER at different frequencies

(b) BER at different volumetric water contents

(c) BER at different transmit powers, $\theta = 25\%$

(d) BER at different transmit powers, $\theta = 50\%$

Figure 7. Bit error rates (Receiver on seabed and sender at various depths).

[6] Crossbow, "Mica2, micaz and iris motes," [Online]. Available: http://www.xbow.com [Accessed: January 20, 2010].

[7] A. R. Silva and M. C. Vuran, "Empirical evaluation of wireless underground-to-underground communication in wireless underground sensor networks," in *DCOSS 2009, LNCS 5516*, B. K. et al., Ed. Springer-Verlag, 2009, pp. 231–244.

[8] WFS Technologies, "Through-water and through-ground communication, sensing and navigation technology," [Online]. Available: http://www.wirelessfibre.co.uk [Accessed: January 20, 2010].

[9] Radiometrix, "Wireless data transmission," [Online]. Available: http://www.radiometrix.com [Accessed: January 29, 2010].

[10] M. T. Hallikainen, F. T. Ulaby, M. C. Dobson, M. A. EL-Rayes, and L.-K. Wu, "Microwave dielectric behavior of wet soil - part i: Empirical models and experimental observations," *IEEE Trans. on Geoscience and Remote Sensing*, vol. GE-23, no. 1, pp. 25–34, Jan. 1985.

[11] N. R. Peplinski, F. T. Ulaby, and M. C. Dobson, "Dielectric properties of soils in the 0.3-1.3-ghz range," *IEEE Trans. on Geoscience and Remote Sensing*, vol. 33, no. 3, pp. 803–807, May 1995.

[12] G. Topp, J. Davies, and A. Annan, "Electromagnetic determination of soil water content: measurements in coaxial transmission lines." *Water Resources Research*, vol. 16, no. 3, pp. 574–582, 1980.

[13] M. C. Dobson, F. T. Ulaby, M. T. Hallikainen, and M. A. EL-Rayes, "Microwave dielectric behavior of wet soil - part ii: Dielectric mixing models," *IEEE Trans. on Geoscience and Remote Sensing*, vol. GE-23, no. 1, pp. 35–46, Jan. 1985.

[14] T. Kelleners, D. Robinson, P. Shouse, J. Ayars, and T. Skaggs, "Frequency dependence of the complex permittivity and its impact on dielectric sensor calibration in soils," *Soil Science Society of America Journal*, no. 69, pp. 67–76, 2005.

[15] "The qualnet simulator," [Online]. Available: http://www.scalable-networks.com/products/developer.php [Accessed: July 31, 2009].